# Efficient Substitutional Photochemistry of a Third-Row Transition Metal β-Diketonate Complex

**Richard J. Lavallee,[†] Bentley J. Palmer,[†] Roland Billing,[‡] Horst Hennig,[‡] Guillermo Ferraudi,[§] and Charles Kutal*,[†]**

Department of Chemistry, University of Georgia, Athens, Georgia 30602, Institut für Anorganische Chemie, Universität Leipzig, 04103 Leipzig, Germany, and Radiation Laboratory, University of Notre Dame, Notre Dame, Indiana 46556

*Received May 1, 1997*[⊗]

Ultraviolet irradiation of $Pt(acac)_2$ ($acac^-$ is the anion of acetylacetone) in nonaqueous solvents results in competing photochemical processes whose relative importance depends upon the solution environment. In $CH_3CN$ containing a strong protonic acid, the complex undergoes clean, irreversible substitution of an $acac^-$ ligand by solvent to yield $Pt(acac)(CH_3CN)_2^+$ and free H(acac). The quantum yield for this process is high (∼0.3) and independent of the irradiation wavelength, presence of dissolved oxygen, incident light intensity, acid concentration ($(1-50) \times 10^{-3}$ M), and temperature. The primary photochemical step has been identified as heterolytic cleavage of a Pt−O bond to yield an intermediate, $\mathbf{I_1}$, formulated as a Pt(II) complex containing a monodentate O-bonded $acac^-$ ligand and a coordinated solvent molecule. Protonation of this monodentate ligand labilizes the remaining bond to the metal and facilitates loss of H(acac). In nonacidified $CH_3CN$, $\mathbf{I_1}$ undergoes rechelation of the dangling $acac^-$ ligand to regenerate $Pt(acac)_2$ in competition with secondary photolysis to form a complicated mixture of products. Photolysis in $CH_2Cl_2$ and $CH_3OH$ results in inefficient redox decomposition of $Pt(acac)_2$ to yield Pt metal and free H(acac). The role of solvent in determining the relative importance of photosubstitution vs photoredox decomposition is discussed. In addition, the mechanism by which $Pt(acac)_2$ functions as a photoinitiator for the anionic polymerization of a 2-cyanoacrylate is reconsidered in light of the present study.

## Introduction

Several studies have yielded information about the photoreactivity patterns of first- and second-row transition metal β-diketonate complexes of general formula $M(dik)_n$ (dik denotes the monoanion of a 1,3-diketone and $n = 2$ or 3).[1] Photoexcitation of a complex to a ligand-to-metal charge transfer (LMCT) excited state formally generates a reduced metal center bound to a β-diketone radical. As summarized in eq 1 for a

$$M^{III}(dik)_3 \underset{(i)}{\overset{h\nu}{\rightleftharpoons}} M^{II}(dik)_2(dik^{\cdot}) \begin{cases} \xrightarrow[(ii)]{} M^{III}(dik)_3 \text{ (isomer)} \\ \xrightarrow[(iii)]{SH} M^{II}(dik)_2 + H(dik) + S^{\cdot} \end{cases} \quad (1)$$

trischelate complex, this reactive species may undergo (i) back electron transfer to regenerate the parent complex, (ii) back electron transfer accompanied by rearrangement to yield an optical, geometrical, or linkage isomer, or (iii) scavenging of the ligand radical by a hydrogen atom donor, SH, to produce free β-diketone and the one-electron-reduced complex. The relative contributions of these competing pathways depend upon the metal, ligand, and solvent. In contrast to LMCT states, the ligand field states of β-diketonate complexes appear to be unreactive. The sole exception is chromium(III), whose complexes undergo stereochemical rearrangement with modest quantum efficiency (∼$10^{-3}$) following ligand field excitation.[2,3]

Recently, we reported that $Pt(acac)_2$ ($acac^-$ is the anion of acetylacetone) functions as an effective photoinitiator for the

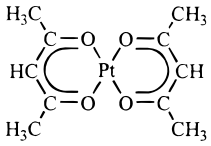

$Pt(acac)_2$

anionic polymerization of a 2-cyanoacrylate monomer.[4] Preliminary experiments aimed at delineating the mechanism of photoinitiation suggested that irradiation of the complex induces the heterolytic cleavage of a Pt−O bond and consequent substitution of one $acac^-$ ligand by solvent. Since efficient photosubstitution had not been observed previously for transition metal β-diketonate complexes, we undertook a detailed study of the solution photochemistry of $Pt(acac)_2$. Our results, described in full below, establish the importance of heterolytic metal−ligand bond rupture and the key role played by the solution environment in the photosubstitutional chemistry of this third-row transition metal complex. The present study complements the recent work of Lewis et al. on the spectroscopy and photochemistry of $Pt(dik)_2$ complexes[5] and their use as photoactivated hydrosilation catalysts.[6] In addition, it provides a straightforward explanation for the behavior of $Pt(acac)_2$ as an anionic photoinitiator.

* Corresponding author.
[†] University of Georgia.
[‡] Universität Leipzig.
[§] University of Notre Dame.
[⊗] Abstract published in *Advance ACS Abstracts,* November 1, 1997.

(1) Comprehensive reviews: (a) Lintvedt, R. L. In *Concepts of Inorganic Photochemistry*; Adamson, A. W., Fleischauer, P., Eds.; John Wiley: New York, 1975; Chapter 7. (b) Marciniak, B.; Buono-Core, G. E. *J. Photochem.* Photobiol., *A* **1990**, *52*, 1.
(2) Stevenson, K. L.; vanden Driesche, T. P. *J. Am. Chem. Soc.* **1974**, *96*, 7964.
(3) Kutal, C.; Yang, D. B.; Ferraudi, G. *Inorg. Chem.* **1980**, *19*, 2907.
(4) Palmer, B. J.; Kutal, C.; Billing, R.; Hennig, H. *Macromolecules* **1995**, *28*, 1328.
(5) Lewis, F. D.; Miller, A. M.; Salvi, G. D. *Inorg. Chem.* **1995**, *34*, 3173.
(6) Lewis, F. D.; Salvi, G. D. *Inorg. Chem.* **1995**, *34*, 3182.

S0020-1669(97)00515-6 CCC: $14.00 

## Experimental Section

**A. Reagents.** Commercially-available $Pt(acac)_2$ (Johnson Matthey) was shown to be analytically pure by elemental analysis and $^1H$ NMR spectroscopy. Acetonitrile (Baker HPLC grade) and methanol (Baker reagent grade) were used as received for spectroscopic and photochemical experiments. Methanesulfonic acid (MSA), acetylacetone, and $CD_3CN$ were purchased (Aldrich) in the highest purity available and used as received. $[Pt(acac)(CH_3CN)_2]CH_3SO_3$ was prepared by irradiating (>290 nm) an $CH_3CN$ solution of $Pt(acac)_2$ and a slight excess of MSA until the parent complex was completely consumed. Solvent was removed by rotary evaporation, and the remaining volatile components, acetylacetone and MSA, were removed *in vacuo* overnight. Any remaining acid impurities were removed by washing the product with diethyl ether. The resulting pale yellow solid was characterized by $^1H$ and $^{13}C$ NMR spectroscopy, electronic spectroscopy, and elemental analysis (Atlantic Microlab, Inc.). Anal. Calcd for $C_{10}H_{16}N_2O_5SPt$: C, 25.48; H, 3.42; N, 5.94. Found: C, 25.20; H, 3.45; N, 5.83.

**B. Instrumentation.** Electronic absorption spectra were recorded on a Varian DMS 300 spectrophotometer. High-performance liquid chromatography (HPLC) experiments were performed on an apparatus consisting of a Thermo Separation Products Constametric 4100 Bio/MS (20 $\mu$L sample loop volume), a Thermo Separation Products 3200 Spectromonitor operating at 220 nm, and a Hamilton PRP-1 reversed-phase column (25 × 0.41 cm). The mobile phase consisted initially of an 80:20 (v/v) mixture of water/acetonitrile which was linearly ramped to 0:100 water/acetonitrile over a period of 20 min, with a flow rate of 0.8 mL/min. Chromatograms were recorded on a Chromjet integrator. Room-temperature $^1H$ and proton-decoupled $^{13}C$ NMR spectra were obtained on Bruker AC-250 and AC-300 spectrometers operating at 250.134 and 300.135 MHz, respectively. Proton spectra at 10 °C were measured on a Bruker AMX-400 spectrometer operating at 400.137 MHz. Solvent ($CD_3CN$) chemical shifts were referenced to internal tetramethylsilane (TMS) at 0 ppm, and in all subsequent experiments signals were referred to TMS by assigning the solvent multiplet a value of 1.95 ($^1H$) or 1.3 ($^{13}C$) ppm. Typical solution concentrations for HPLC and NMR experiments were $2 \times 10^{-3}$ M or saturated.

Continuous-photolysis experiments at 254 nm utilized a low-pressure mercury lamp situated 2 cm from the sample. Irradiations at other wavelengths were conducted with a high-pressure mercury-arc lamp located 34 cm from the sample. Interference filters with widths at half-height of 12 and 25 nm were used to isolate the 313- and 365-nm mercury lines, respectively. Incident-light intensities at each wavelength were measured with the ferrioxalate actinometer.[7] Polychromatic (>290 nm) irradiations were performed by passing the full output of the high-pressure lamp through a water-filled Pyrex cell placed in front of the sample.

**C. Photochemical Studies.** Solutions of $Pt(acac)_2$ were irradiated with stirring in 1-cm rectangular quartz cells maintained at either 10 or 25 °C in a thermostated holder. In some runs, the solutions were deoxygenated by bubbling with argon for 30 min prior to photolysis. Photosubstitution quantum yields ($\Phi_{sub}$) in $CH_3CN$ containing MSA were determined spectroscopically by monitoring the absorbance decrease at 390 nm, a wavelength at which the extinction coefficients of the parent complex and the photoproduct, $Pt(acac)(CH_3CN)_2^+$, are 1160 and 36 $M^{-1}$ $cm^{-1}$, respectively. Typical $Pt(acac)_2$ concentrations in these experiments were $(2.0-5.0) \times 10^{-4}$ M, and samples were photolyzed to less than 30% reaction. Corrections for inner-filter effects were applied when necessary. Photosubstitution quantum yields in $CH_3OH$ were determined by a similar procedure. While the absorbances of the likely Pt(II) photoproduct ($Pt(acac)(CH_3OH)_2^+$) at the excitation and monitoring wavelengths were not determined, the constancy of $\Phi_{sub}$ at different extents of photolysis (3−17%) indicates that inner-filter and secondary-photolysis effects arising from this species can be neglected. Since $\Phi_{sub}$ exhibits a dependence upon acid concentration, the limiting quantum yield at a specific excitation wavelength was calculated from the *y* intercept of a plot of $1/\Phi_{sub}$ vs 1/[MSA]. Photosubstitutional loss of $acac^-$ from $Pt(acac)(CH_3CN)_2^+$ in acidified $CH_3CN$ was determined by monitoring the decrease in sample absorbance at 390 nm. Here also, the limiting quantum yield was obtained from a plot of $1/\Phi_{sub}$ vs 1/[MSA].

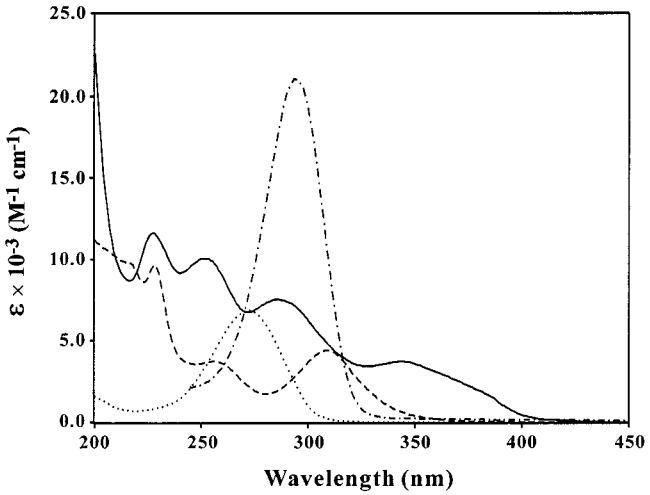


**Figure 1.** Electronic absorption spectra in $CH_3CN$: (—) $Pt(acac)_2$; (---) $Pt(acac)(CH_3CN)_2^+$; (•••) H(acac); (•—•) $acac^-$.

Thermal reactions of the photoproducts in $CH_3CN$ at 22 °C were monitored on a Shimadzu UV-3101 PC spectrometer that utilized a kinetics software package. In these experiments, solutions of $Pt(acac)_2$ were irradiated for various times with Pyrex-filtered light; absorbance changes at 365 nm were then followed as a function of time, beginning 10 s after the cessation of photolysis. For the identification of photoproducts by NMR spectroscopy, solutions of $Pt(acac)_2$ were photolyzed in spectrophotometer cells with Pyrex-filtered light and then transferred to NMR tubes. Typically, spectra were acquired within 5 min of irradiation.

## Results and Discussion

**A. Spectral Considerations.** The electronic absorption spectra of H(acac), $acac^-$, and $Pt(acac)_2$ in room-temperature $CH_3CN$ are compared in Figure 1. The single band observed at 272 nm for H(acac) has been assigned to a $\pi-\pi^*$ (HOMO → LUMO) transition of the enol tautomer.[8] Deprotonation of the $\beta$-diketone with a 10-fold molar excess of KOH (added as a methanol solution) yields $acac^-$, which exhibits a more intense $\pi-\pi^*$ band at 294 nm. Square-planar $Pt(acac)_2$ displays four distinct bands at 227, 252, 285, and 343 nm and discernible shoulders at ∼384 and ∼421 nm. On the basis of a semi-empirical molecular orbital treatment, Lewis et al. proposed that the 343-nm band and one of the higher-energy bands arise from symmetry-allowed $\pi-\pi^*$ transitions localized on the $\beta$-diketonate ligands.[9] No assignments have yet been offered for the two low-energy shoulders. In their spectral analysis of $Pt(hfacac)_2$ ($hfacac^-$ is the anion of hexafluoroacetylacetone), Reber and Zink attributed bands at 435 and 454 nm (in cyclohexane) to LMCT and ligand field transitions, respectively.[10] A LMCT assignment for the 384-nm shoulder in the spectrum of $Pt(acac)_2$ seems implausible, since the absence of the highly electron-withdrawing fluorine atoms on the ligands should shift such a transition to lower, not higher, energy. Assignment of the 421-nm and, probably, the 384-nm shoulders as ligand field transitions appears to be more reasonable, since low-intensity ($\epsilon \sim 10^2$) d−d transitions commonly appear in the near-UV−visible region for Pt(II) complexes containing

(7) Hatchard, C. G.; Parker, C. A. *Proc. R. Soc. London, Ser. A* **1956**, *235*, 518.

(8) Nakanishi, H.; Morita, H.; Nagakura, S. *Bull. Chem. Soc. Jpn.* **1977**, *50*, 2255.

(9) Lewis, F. D.; Salvi, G. D.; Kanis, D. R.; Ratner, M. A. *Inorg. Chem.* **1993**, *32*, 1251.

(10) Reber, C.; Zink, J. I. *Inorg. Chem.* **1992**, *31*, 2786.

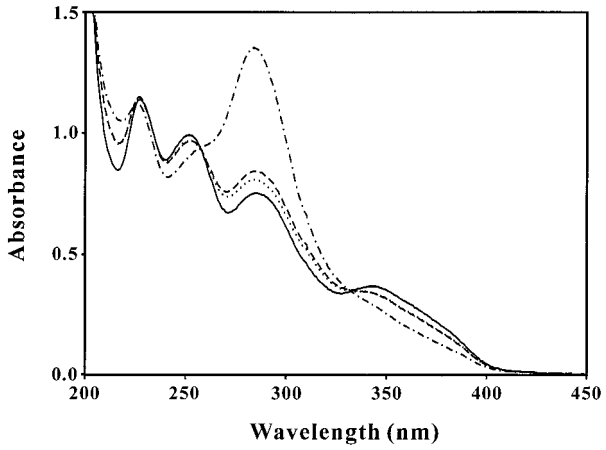


**Figure 2.** Spectral changes upon irradiating $Pt(acac)_2$ in $CH_3CN$ at 10 °C: (—) sample before irradiation; (·—·) irradiated at 365 nm for 75 s, spectrum taken 45 s after cessation of photolysis; (---) photolyte 3.37 min after cessation of photolysis; (···) photolyte 2 h after cessation of photolysis.

ligands low in the spectrochemical series.[11] We shall revisit this question after considering the photochemical behavior of $Pt(acac)_2$.

**B. Photochemical Studies in the Absence of Acid.** Preliminary experiments revealed that $Pt(acac)_2$ undergoes inefficient photochemistry when irradiated at 365 nm in room-temperature methanol and dichloromethane. Disappearance quantum yields, estimated by monitoring the decrease in the long-wavelength absorption band of the complex immediately (<1 min) after photolysis, are $6 \times 10^{-3}$ and $<10^{-5}$, respectively. Deoxygenating the solution by bubbling with argon has no noticeable effect upon the photochemical behavior. Prolonged photolysis results in the appearance of a band at ~272 nm characteristic of free H(acac) and featureless absorption tailing from the deep-UV into the visible region attributable to scattering from a colloidal suspension. Similar spectral behavior was reported by Lewis et al., who identified the colloid as metallic platinum.[5] Collectively, these results indicate that the dominant photoinduced reaction of $Pt(acac)_2$ in weakly coordinating solvents is redox decomposition (eq 2; other products arise from the oxidation of a ligand and/or a molecule of solvent).

$$Pt(acac)_2 \xrightarrow[CH_2Cl_2]{h\nu} Pt + H(acac) + \text{other products} \qquad (2)$$

Quite different behavior obtains upon 365-nm irradiation of the complex in $CH_3CN$ at 25 °C. The disappearance quantum yield measured immediately after photolysis increases to $>10^{-2}$, and the observed spectral changes (vide infra) suggest a reaction other than redox decomposition. These spectral changes are partially reversible in the dark over a period of a few min, indicating that the initial photoproduct(s) can thermally regenerate the parent complex in this time frame. Because of this rapid back-reaction, the quoted value of the disappearance quantum yield represents only an approximate measure of the photosensitivity of the complex. Further experiments were conducted at 10 °C in order to slow the back-reaction and allow more convenient monitoring of the system. As seen in Figure 2, the photoinduced bleaching of the 343-nm band is accompanied by the appearance of a band at $283 \pm 1$ nm which we attribute to the formation of an intermediate $\mathbf{I_1}$. Within 3 min after the cessation of irradiation, this new band decreases sharply in intensity, while ~50% of the starting material is regenerated. Subsequent spectral changes include a slow decrease in intensity and slight blue shift of a feature at 280 nm along with a very small increase in the long-wavelength absorbance.

(11) Balzani, V.; Carassiti, V. *Photochemistry of Coordination Compounds*; Academic Press: New York, 1970; Chapter 12.

**Table 1.** Extent of Thermal Back-Reaction in a Photolyzed Solution of $Pt(acac)_2$ in $CH_3CN$ at 22 °C

| irradn time (min) | % reacn[a] | % recovery[b] | irradn time (min) | % reacn[a] | % recovery[b] |
|---|---|---|---|---|---|
| 0.16 | 5.8 | 99.8 | 3.0 | 10.4 | 49.3 |
| 0.50 | 9.0 | 91.6 | 4.0 | 11.7 | 45.4 |
| 1.0 | 8.0 | 81.8 | 10.0 | 18.2 | 23.1 |
| 2.0 | 9.5 | 62.2 | 20.0 | 29.7 | 13.3 |

[a] Percent of $Pt(acac)_2$ photolyzed, as measured by the decrease in absorbance at 365 nm 10 s after the cessation of irradiation. [b] Percent of photolyzed material that regenerates $Pt(acac)_2$, as measured by the absorbance at 365 nm 5 min after the cessation of irradiation.

The nature of the thermal back-reaction was investigated in a series of experiments that involved irradiating $CH_3CN$ solutions of $Pt(acac)_2$ with polychromatic light for various times and monitoring the recovery of the absorbance at 365 nm. Most of the recovery occurred within the first 30 s at 22 °C, followed by a period of much slower change. As shown in Table 1, the extent of recovery is highly dependent on the length of irradiation. While essentially complete regeneration of $Pt(acac)_2$ occurs at low photochemical conversions, the sharp decrease in the percent recovery at higher conversions signals the existence of a competitive pathway that leads to permanent products and depends upon the concentration of $\mathbf{I_1}$. We have considered two possibilities for this pathway. The first involves thermal aggregation of $\mathbf{I_1}$ to yield oligomeric products; this process should assume increasing importance as the concentration of metastable $\mathbf{I_1}$ builds during the course of photolysis. Alternatively, permanent product formation could result from secondary photolysis of $\mathbf{I_1}$; this process also should become more prominent at higher photochemical conversions owing to the increasing fraction of the incident radiation absorbed by $\mathbf{I_1}$. Measuring the disappearance quantum yield of $Pt(acac)_2$ as a function of sample absorbance offers an experimental basis for distinguishing between these two possibilities. We expect thermal aggregation to become relatively more important as the absorbance of the starting complex increases (e.g., from 0.29 to 3.7), since the larger number of photons absorbed by the optically dense sample generates a higher concentration of $\mathbf{I_1}$. By contrast, secondary photolysis, being a two-photon (or more) process, should become more important at low absorbance owing to less competitive absorption by unreacted $Pt(acac)_2$. The finding that the disappearance quantum yield at 365 nm increases as sample absorbance decreases constitutes strong evidence that secondary photolysis of $\mathbf{I_1}$ is the dominant pathway leading to permanent photoproducts.

Identification of photoproducts was facilitated by the use of NMR spectroscopy. Table 2 provides a compilation of NMR data for several key species considered in the ensuing discussion. A nonirradiated solution of $Pt(acac)_2$ in $CD_3CN$ gives rise to two $^1H$ signals at 1.87 and 5.62 ppm, assignable to the methyl and methine protons, respectively, of the acetylacetonate ligands. The spectrum of an argon-bubbled solution exposed to Pyrex-filtered light at 25 °C is extremely complex, exhibiting at least 16 new signals in the 6.4−4.6 ppm region, 5 new signals in the 4.6−3.0 ppm region, and a multitude of new signals in the 3.0−1.4 ppm region. Varying the excitation wavelength, oxygen content of the sample, or the temperature has no significant effect upon the spectral features observed. All signals appear to be singlets, but extensive overlap in the methyl region complicates the analysis. The two most intense signals appear

**Table 2.** Summary of $^1$H and $^{13}$C NMR Data for Pt(acac)$_2$, Pt(acac)(CH$_3$CN)$_2^+$, and the Keto and Enol Tautomers of Acetylacetone

| | $\delta_{^1H}$ (ppm) | | $\delta_{^{13}C}$ (ppm) | | |
|---|---|---|---|---|---|
| | −CH$_3$ | −CH═(−CH$_2$−) | −CH$_3$ | −CH═(−CH$_2$−) | CO |
| Pt(acac)$_2$ | 1.87 | 5.62 | 25.5, $J$ = 40 Hz[b] | 103.4, $J$ = 74 Hz[b] | 186.8 |
| Pt(acac)(CH$_3$CN)$_2^+$ | 2.02[a] | 5.88 | 25.1,[a] $J$ = 43 Hz[b] | 103.9, $J$ = 68 Hz[b] | 187.1 |
| enol acetylacetone | 2.03 | 5.62 | 24.9 | 101.1 | 192.7 |
| keto acetylacetone | 2.15 | (3.61) | 31.0 | (58.6) | 205.0 |

[a] Methyl signal of coordinated acetylacetonate. The methyl resonance of coordinated CH$_3$CN appears at 2.70 ppm ($^1$H) and 4.4 ppm ($^{13}$C). [b] $J$ values denote $^{195}$Pt−$^{13}$C spin−spin coupling constants.

at 5.88 and 3.61 ppm; the latter is assigned to the methylene protons of the keto tautomer of acetylacetone by comparison with an authentic sample. HPLC experiments are consistent with the NMR results, as at least nine new chromatographic peaks are detected in the photolyte. Both techniques also reveal the occurrence of slow thermal reactions in a photolyzed solution as evidenced by changing peak areas over the course of 24 h. Extensive photolysis of the concentrated samples required for the NMR studies results in a darkening of the solution and eventual deposition of a brown film on the walls of the container. This film is soluble in pyridine and concentrated hydrochloric acid and therefore cannot be metallic platinum. The presence of numerous closely-spaced peaks superimposed upon a rising baseline in the methyl and methine regions of the NMR spectra of extensively photolyzed solutions is consistent with the formation of oligomeric species containing Pt(acac) units. Attempts to characterize these species by electrospray ionization mass spectrometry were unsuccessful.

**C. Photochemical Studies in the Presence of Acid.** Our previous observation[4] that MSA inhibits anionic photoinitiation by Pt(acac)$_2$ led us to investigate the effect of this strong acid upon the photochemistry of the complex in CH$_3$CN. Irradiation of an acidified solution with 365-nm light at 25 °C causes a reduction in intensity of the long-wavelength absorption band, the appearance of a shoulder at ∼309 nm, and the appearance of a band at ∼270 nm attributable to free H(acac). Over the course of 30 min in the dark, further spectral changes are limited to a decrease in intensity and slight blue shift of the 270-nm band, which results from equilibration of the keto and enol tautomers of H(acac). Most importantly, failure of the 343-nm band to increase in intensity during this period establishes that regeneration of Pt(acac)$_2$ has been inhibited by the acid. As shown in Figure 3, irradiation at 10 °C initially results in the appearance of a very broad, composite feature centered at ∼285 nm which we attribute to the formation of an intermediate **I$_2$**. This feature thermally evolves into the 270-nm band within 4 min. The latter process is accompanied by the growth of a sharp band at 228 nm and the appearance of the shoulder at 309 nm. Further spectral changes mimic those observed at 25 °C. Analysis of the photolyte by HPLC shows that the photochemistry of Pt(acac)$_2$ in CH$_3$CN is much cleaner in the presence of acid, as only two new peaks were detected after irradiation. One of these peaks is easily identified as H(acac), while the other is attributed to a Pt-containing photoproduct, **P**, the detailed characterization of which is discussed below.

The interrelationship of intermediates **I$_1$** and **I$_2$** was probed by irradiating Pt(acac)$_2$ in CH$_3$CN at 10 °C, adding MSA to the photolyte immediately after photolysis, and then monitoring the spectral changes that occur in the dark over time. As seen in Figure 4, the initial spectrum after addition of acid exhibits a prominent band at ∼292 nm. During the next 20 min, the disappearance of this band is accompanied by the growth of a band at ∼256 nm and the appearance of shoulders at ∼272 and ∼309 nm. These spectral changes combine features seen during the photolyses of Pt(acac)$_2$ in the absence (Figure 2) and

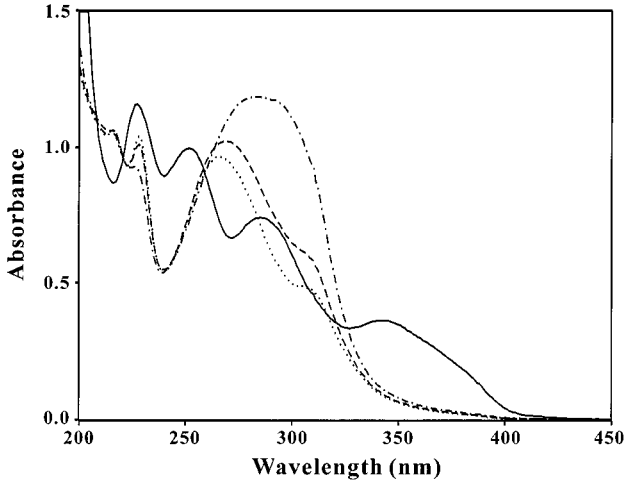


**Figure 3.** Spectral changes upon irradiating Pt(acac)$_2$ in CH$_3$CN containing 1.0 × 10$^{-3}$ M MSA at 10 °C: (—) sample before irradiation; (•—•) sample irradiated at 365 nm for 75 s, spectrum taken 45 s after cessation of photolysis; (---) photolyte 2.75 min after cessation of photolysis; (•••) photolyte 30 min after cessation of photolysis.

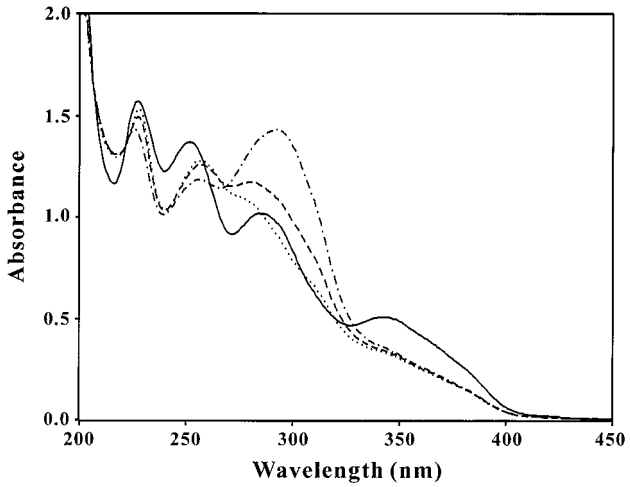


**Figure 4.** Spectral changes upon irradiating Pt(acac)$_2$ in CH$_3$CN at 10 °C: (—) sample before irradiation; (•—•) sample irradiated at 365 nm for 75 s followed by addition of 1.0 × 10$^{-3}$ M MSA, spectrum taken 45 s after cessation of photolysis; (---) photolyte containing acid 3.75 min after cessation of photolysis; (•••) photolyte containing acid 20 min after cessation of photolysis.

presence (Figure 3) of MSA. We conclude from such behavior that **I$_1$** can be transformed into **I$_2$** under acidic conditions.

The $^1$H NMR spectra of acidified solutions irradiated with 365-nm or Pyrex-filtered light contain five new major signals at 2.02, 2.03, 2.15, 3.61, and 5.88 ppm. In addition, two minor peaks appear in the region between 5.65 and 5.85 ppm and two other minor peaks occur around 1.90 ppm. Neither of the former pair appears in the absence of MSA. Comparison to the spectrum of free H(acac) allows assignment of the signals at 2.03, 2.15, and 3.61 ppm to the methyl protons of the enol tautomer, the methyl protons of the keto tautomer, and the

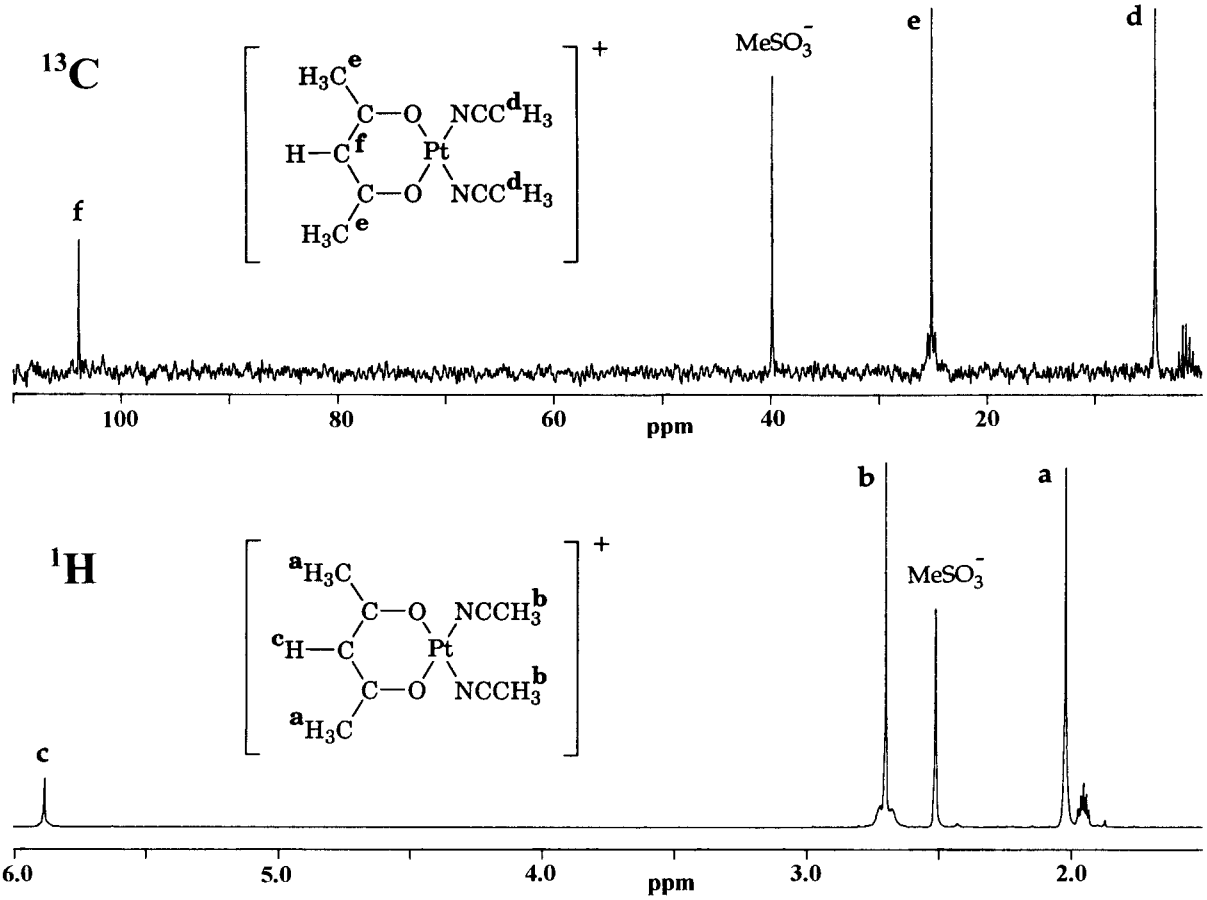


**Figure 5.** $^1$H (lower) and proton-decoupled $^{13}$C (upper) NMR spectra of Pt(acac)$(CH_3CN)_2^+$ (as its $CH_3SO_3^-$ salt) in $CD_3CN$. $^{13}$C signals due to quartenary carbons of coordinated acac$^-$ are not shown. Multiplets at 1.95 ppm in the $^1$H spectrum and at 1.3 ppm in the $^{13}$C spectrum arise from solvent impurities.

methylene protons of the keto tautomer, respectively (Table 2). It should be noted that the methine proton of the enol tautomer resonates at 5.62 ppm, thus making it degenerate with the methine proton signal of Pt(acac)$_2$. The two remaining signals at 2.02 and 5.88 ppm are assigned to a major photoproduct, **P**, formulated as a square-planar Pt-containing species containing one bidentate acetylacetonate ligand and two coordinated solvent molecules, Pt(acac)$(CH_3CN)_2^+$. Significant baseline broadening of both signals results from unresolved $^{195}$Pt$-^1$H coupling. Such broadening also is present in the spectrum of Pt(acac)$_2$ but is notably absent in the spectrum of H(acac). High-resolution spectra reveal a $^{195}$Pt$-^1$H coupling constant of 8.0 Hz for the 5.88 ppm signal of Pt(acac)$(CH_3CN)_2^+$, a value comparable to those found for other Pt complexes containing one bidentate acetylacetonate ligand.[12,13]

The $^{13}$C NMR spectrum of the photolyte provides additional support for the formation of Pt(acac)$(CH_3CN)_2^+$. In addition to resonances attributable to free H(acac), signals appear at 25.1, 103.9, and 187.1 ppm corresponding to the methyl, methine, and carbonyl carbons, respectively, of the Pt-containing photoproduct. Both the methyl and methine signals exhibit the characteristic 1:4:1 splitting due to $^{195}$Pt$-^{13}$C coupling, confirming the presence of Pt in this complex. Coupling constants (Table 2) agree well with values found in the literature[14] and are on the same order as those for Pt(acac)$_2$. No Pt splitting is detectable for the carbonyl carbons in Pt(acac)$(CH_3CN)_2^+$ owing to problems with carbon sensitivity at the concentrations employed.

**D. Properties of Pt(acac)$(CH_3CN)_2^+$.** An authentic sample of Pt(acac)$(CH_3CN)_2^+$ was synthesized by exhaustive photolysis of Pt(acac)$_2$ in $CH_3CN$ containing a slight excess of MSA to scavenge acac$^-$. The complex, isolated as the methanesulfonate salt, is air and/or heat sensitive, decomposing within 1 day at room temperature to a gray, malodorous solid. Further decomposition produces an intensely blue material that is insoluble in acetone, acetonitrile, and chloroform but soluble in water. The complex remains intact for up to 2 weeks, however, when stored in a freezer under nitrogen.

The $^1$H NMR spectrum of Pt(acac)$(CH_3CN)_2^+$ in $CD_3CN$ (Figure 5) exhibits signals due to the methine (5.88 ppm) and methyl (2.02 ppm) protons of acetylacetonate and the protons of acetonitrile (2.70 ppm). Integration of the areas of these signals gives the expected 1:6:6 relationship, thereby confirming the presence of two coordinated solvent molecules in the complex. The coordinated solvent resonance shows clear $^{195}$Pt splitting with a $^{195}$Pt$-^1$H coupling constant of 11 Hz. In contrast to its limited solid-state stability, the complex is indefinitely stable in acetonitrile solution shielded from light. Over a period of weeks, $^1$H NMR spectral changes are limited to thermal solvent exchange as evidenced by the decrease in area of the coordinated solvent signal and the appearance of free $CH_3CN$. The pseudo-first-order rate constant for this process is $(5.8 \pm 0.3) \times 10^{-7}$ s$^{-1}$ at 21 $\pm$ 1 °C, a value consistent with a substitutionally-robust d$^8$ complex. Adding a stoichiometric amount of acac$^-$ (as the K$^+$ salt) to an $CH_3CN$ solution of Pt(acac)$(CH_3CN)_2^+$ does not lead to regeneration of Pt(acac)$_2$ for up to 4 h at room temperature. This negative result argues against the bimolecular recombination of these oppositely

(12) Lewis, J.; Long, R. F.; Oldham, C. *J. Chem. Soc.* **1965**, 6740.
(13) Holloway, C. E.; Hulley, G.; Johnson, B. F. G.; Lewis, J. *J. Chem. Soc. A* **1970**, 1653.
(14) Wilkie, C. A.; Haworth, D. T. *J. Inorg. Nucl. Chem.* **1978**, *40*, 195.

**Table 3.** Photosubstitution Quantum Yields for $Pt(acac)_2$ in $CH_3CN$ Containing $1.0 \times 10^{-3}$ M Methanesulfonic Acid

| run | $\lambda_{excit}$ (nm) | temp (°C) | argon purged | intensity (einstein/s $\times 10^8$) | $\Phi_{sub}$[a,b] |
|---|---|---|---|---|---|
| 1 | 254 | 25 | no | 1.96 | $0.27 \pm 0.01$ (2) |
| 2 | 254 | 25 | yes | 1.96 | $0.30 \pm 0.00$ (2) |
| 3 | 313 | 25 | no | 1.26 | $0.27 \pm 0.02$ (6) |
| 4 | 313 | 25 | yes | 1.24 | $0.28 \pm 0.01$ (2) |
| 5 | 365 | 25 | no | 6.28 | $0.36 \pm 0.02$ (2) |
| 6 | 365 | 25 | yes | 6.28 | 0.35 (1) |
| 7 | 365 | 25 | no | 3.00 | 0.37 (1) |
| 8 | 365 | 10 | no | 5.58 | $0.31 \pm 0.01$ (4) |
| 9 | 365 | 25 | no | 2.75 | $0.36 \pm 0.03$[c] (4) |
| 10 | 365 | 25 | no | 3.96 | 0.33[d] (1) |
| 11 | 365 | 25 | no | 3.96 | 0.34[e] (1) |

[a] $[Pt(acac)_2] = (2.0-5.0) \times 10^{-4}$ M unless otherwise indicated. [b] Error limits represent deviation from the mean of two or more runs; number of runs is indicated in parentheses. We estimate the accuracy of the quantum yields to be ±10%. [c] Solution contains $5.1 \times 10^{-2}$ M MSA. [d] $[Pt(acac)_2] = 1.0 \times 10^{-4}$ M; initial absorbance at $\lambda_{excit}$ was 0.29. [e] $[Pt(acac)_2] = 1.9 \times 10^{-3}$ M; initial absorbance at $\lambda_{excit}$ was ~5.6.

charged species as the cause of the rapid thermal back-reaction occurring in photolyzed solutions in the absence of acid.

The electronic absorption spectrum of $Pt(acac)(CH_3CN)_2^+$ in $CH_3CN$ exhibits bands at 228, 256, and 309 nm (Figure 1). The last feature accounts for the appearance of the shoulder at this wavelength during photolysis of $Pt(acac)_2$ in the presence of acid (Figure 3).

**E. Photoreaction Stoichiometry and Quantum Efficiency.** Photoreaction stoichiometry was elucidated by $^1H$ NMR spectroscopy. A solution of $Pt(acac)_2$ in $CH_3CN$ containing MSA was irradiated, and the concentrations of reactant and photoproducts were determined from the areas of their methine proton signals. After 80% conversion of the starting material, the areas of the keto and enol tautomers of H(acac) and $Pt(acac)(CH_3CN)_2^+$ accounted for 85 ± 5% of the reacted material. Moreover, the areas due to H(acac) and $Pt(acac)(CH_3CN)_2^+$ were equal within 3−7%, demonstrating that these photoproducts are formed in a 1:1 mole ratio. Minor product signals accounted for ~5% of the reacted material, with unobservable products comprising the remainder. After the photolyte had sat in the dark for 72 h, the area of the unreacted starting material was unchanged and the minor products had reacted thermally to yield H(acac) and $Pt(acac)(CH_3CN)_2^+$, which now accounted for 99 ± 5% of the reacted material. Collectively, these results establish that substitution of one $acac^-$ ligand by solvent (eq 3) is the dominant net photoreaction of $Pt(acac)_2$ in acidified $CH_3CN$.

$$Pt(acac)_2 \xrightarrow[CH_3CN]{h\nu,\ H^+} Pt(acac)(CH_3CN)_2^+ + H(acac) \qquad (3)$$

Table 3 contains a summary of photosubstitution quantum yield ($\Phi_{sub}$) data for $Pt(acac)_2$ measured under a variety of experimental conditions in acidified $CH_3CN$. These values were determined by monitoring the photoinduced decrease in absorbance of the long-wavelength absorption band of the complex (e.g., Figure 3). The data reveal that photosubstitution occurs with high quantum efficiency and has no significant wavelength dependence over the range 254−365 nm (compare runs 1, 3, and 5 or runs 2, 4, and 6). Moreover, $\Phi_{sub}$ is insensitive to the presence of dissolved oxygen (runs 1 and 2, runs 3 and 4, or runs 5 and 6), a 50-fold increase in acid concentration (runs 5 and 9), light intensity (runs 5 and 7), temperature (runs 8 and 9), and the initial absorbance of the sample (runs 10 and 11). The last result indicates that secondary photolysis does not play an important role in the substitutional photochemistry of $Pt(acac)_2$ in the presence of acid.

**Scheme 1**

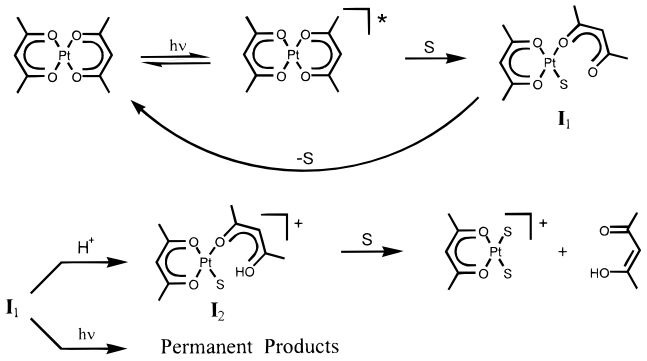


Photolysis of $Pt(acac)_2$ in $CH_3OH$ containing $(1-77) \times 10^{-3}$ M MSA leads to spectral changes very similar to those observed in acidified $CH_3CN$ (Figure 3). While detailed product analyses were not performed, this finding suggests that the complex undergoes photosubstitution of an $acac^-$ ligand by solvent to yield $Pt(acac)(CH_3OH)_2^+$ and H(acac). For 365-nm excitation at 25 °C, $\Phi_{sub}$ attains a limiting value of 0.21 ± 0.02.

The photochemical behavior of $Pt(acac)(CH_3CN)_2^+$ in $CH_3CN$ at 25 °C was investigated briefly. The complex undergoes photosubstitution in the presence of $(1-50) \times 10^{-3}$ M MSA to yield H(acac), identified by its characteristic ultraviolet absorption band, and, most likely, $Pt(CH_3CN)_4^{2+}$ (eq 4). Limiting values of $\Phi_{sub}$ are 0.12 ± 0.02 at 254 nm and 0.18 ± 0.01 at 313 nm.

$$Pt(acac)(CH_3CN)_2^+ \xrightarrow[CH_3CN]{h\nu,\ H^+} Pt(CH_3CN)_4^{2+} + H(acac) \qquad (4)$$

**F. Mechanistic Considerations.** The present study of $Pt(acac)_2$ provides the first example of efficient photosubstitutional chemistry (eq 3) for a transition metal $\beta$-diketonate complex. Moreover, the results reveal that the importance of this pathway relative to competing photoredox decomposition (eq 2) depends upon the solvent. The latter behavior cannot be attributed to varying degrees of solvent coordination to the metal center in ground-state $Pt(acac)_2$, since the electronic absorption spectrum of the complex experiences only minor changes upon switching solvents. Instead, we propose that solvent interacts in a chemically significant manner with the electronically-excited complex and/or a photogenerated intermediate.

Scheme 1 provides a mechanistic framework for discussing the photochemical behavior of $Pt(acac)_2$ in $CH_3CN$. Irradiation of the complex populates a reactive excited state (denoted by an asterisk) that can undergo relaxation to the ground state in competition with heterolytic cleavage of a Pt−O bond to form $\mathbf{I_1}$. We identify $\mathbf{I_1}$ as a Pt(II) complex containing a monodentate O-bonded $acac^-$ ligand and a coordinated solvent molecule, S. The alternative formulation of this intermediate as a complex containing a monodentate C-bonded $acac^-$ ligand is less attractive on kinetic grounds. Species of this type have been reported to persist in solution for hours even at elevated temperatures and, thus, would be too unreactive to account for the short lifetime of $\mathbf{I_1}$. Indeed, one of the minor permanent photoproducts of $Pt(acac)_2$ photolysis in $CH_3CN$ exhibits a methine $^1H$ NMR signal at 4.72 ppm with a $^{195}Pt-^1H$ coupling of 128 Hz. These values fall within the ranges of the chemical

shifts and coupling constants observed for monodentate acac$^-$ ligands C-bonded to Pt(II).[15,16]

The fate of $\mathbf{I_1}$ depends upon the solvent and the extent of reaction. The dominant pathway in pure $CH_3CN$ at low photochemical conversions is rechelation of the dangling acac$^-$ ligand to regenerate Pt(acac)$_2$ (Table 1). At higher conversions, inefficient secondary photolysis of $\mathbf{I_1}$ (disappearance quantum yield $<10^{-2}$ at 25 °C) affords a complicated mixture of products that includes Pt(acac)$(CH_3CN)_2^+$, H(acac), and oligomeric species containing Pt(acac) units. Rapid protonation of $\mathbf{I_1}$ in the presence of acid generates $\mathbf{I_2}$, a species containing a monodentate-bound enol tautomer of acetylacetone. The added proton reduces the basicity of this ligand and thereby facilitates thermal loss of H(acac) to yield Pt(acac)$(CH_3CN)_2^+$ (eq 3). The acid independence of the quantum yield of this photosubstitution process (Table 3) indicates that protons capture all of the $\mathbf{I_1}$ formed in the primary photochemical step. Consequently, $\Phi_{sub}$ provides a good measure of the quantum yield of photoinduced heterolytic Pt−O bond cleavage.

Solvent may play a number of roles in the photochemistry of Pt(acac)$_2$. Minimally, it influences the stability of $\mathbf{I_1}$ by virtue of occupying a coordination site on Pt(II). Weakly-bound solvents such as $CH_2Cl_2$ and $CH_3OH$ should be easily displaced from the metal by the dangling end of the monodentate O-bonded acac$^-$ ligand, and this facile back-reaction results in a short lifetime and low steady-state concentration of the photogenerated intermediate in these media. In contrast, both the lifetime and the concentration of $\mathbf{I_1}$ should increase upon switching to the more strongly-coordinating $CH_3CN$. Under these conditions, secondary photolysis of the intermediate becomes more important and accounts for the higher disappearance quantum yield measured in this solvent. Although not required by our data, another possible role for solvent is associative attack on photoexcited Pt(acac)$_2$. Bond formation between the metal and a good nucleophile such as $CH_3CN$ can stabilize the transition state leading to Pt−O bond cleavage and thereby accelerate the production of $\mathbf{I_1}$. The finding that $\phi_{sub}$ for 365-nm excitation is higher in acidified $CH_3CN$ than in acidified $CH_3OH$ is consistent with this possibility, although the effect (factor of 2) is not large.

Earlier in the discussion, we noted the presence of low-energy ligand field transitions in the electronic absorption spectrum of Pt(acac)$_2$ (Figure 1). Since the excited states that result from such transitions generally are susceptible to heterolytic metal−ligand bond cleavage,[17,18] we suggest that the photosubstitutional chemistry of the complex in $CH_3CN$ originates from a state possessing appreciable ligand field character. Efficient relaxation from higher-lying $\pi-\pi^*$ and (possibly) LMCT excited states would account for the lack of a significant wavelength dependence of $\Phi_{sub}$ (Table 3). Reaction from the latter states may occur, but with very low quantum yield. The inefficient photoredox decomposition of Pt(acac)$_2$ in poorly coordinating solvents may be an example of such a process.

Finally, the mechanism by which Pt(acac)$_2$ functions as a photoinitiator for the anionic polymerization of ethyl 2-cyanoacrylate (CA) can be reconsidered in light of the present results. Previously, we proposed[4] that irradiation of the complex in neat CA releases acac$^-$, which adds to the carbon−carbon double bond of the monomer to yield a resonance-stabilized carbanion (eq 5; X$^-$ is acac$^-$). Polymerization then proceeds

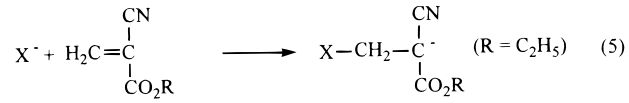

(5)

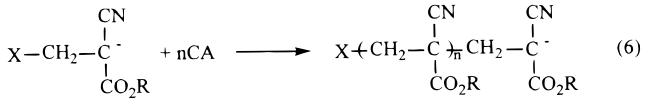

(6)

rapidly by the repetitive addition of monomer units to the growing anionic chain (eq 6). We now know that $\mathbf{I_1}$, a Pt(II) complex containing a monodentate O-bonded acac$^-$ ligand, rather than free acac$^-$, is formed in the primary photochemical step (Scheme 1). Nonetheless, $\mathbf{I_1}$ can serve as a latent source of acac$^-$, as evidenced by the production of H(acac) in the presence of acid. In a process analogous to protonation, electrophilic attack of CA on the dangling end of the monodentate acac$^-$ ligand can produce the carbanion (eq 5) that propagates anionic polymerization.

**G. Concluding Remarks.** Our finding that Pt(acac)$_2$ can undergo efficient photosubstitution of an acac$^-$ ligand by solvent raises an intriguing question: Why are similar pathways not observed for first- and second-row transition metal $\beta$-diketonate complexes? Like Pt(acac)$_2$, these complexes possess low-lying ligand field excited states that should be disposed to heterolytic metal−oxygen bond cleavage which, as depicted in Scheme 1, is the primary photochemical step leading to substitution. Two factors could contribute to this disparity. First, the ligand field states in these lighter metal complexes may be inherently unreactive owing to efficient alternative deactivation pathways. Second, the conditions under which past photochemical studies were conducted may have obscured the occurrence of heterolytic bond cleavage; that is, in the absence of an effective trapping agent for the $\beta$-diketonate anion, the primary products undergo rapid regeneration of the parent complex. Further studies will be required to assess the importance of these factors.

**Acknowledgment.** We thank the National Science Foundation (Grant DMR-9122653 to C.K.) and NATO for financial support.

IC9705150

(15) Gibson, D.; Lewis, J.; Oldham, C. *J. Chem. Soc. A* **1967**, 72.
(16) Ito, T.; Kiriyama, T.; Nakamura, Y.; Yamamoto, A. *Bull Chem. Soc. Jpn.* **1976**, *49*, 3257.
(17) Reference 11, Chapter 6.
(18) Kutal, C.; Adamson, A. W. In *Comprehensive Coordination Chemistry*; Wilkinson, G., Gillard, R. D., McCleverty, J. A., Eds.; Pergamon Press: Elmsford, NY, 1987; Vol. 1, Chapter 7.3.